NMR Microscopy and Image Processing for the Characterization of Flexible Polyurethane Foam

Malgorzata Szayna, Lutz Zedler, and Rüdiger Voelkel*

Dedicated to Professor Quadbeck-Seeger on the occasion of his 60th birthday

Imaging by means of NMR[1] is an established method in the medical field. In materials research, on the other hand, the employment of magnetic resonance for the generation of images is still in the beginning stages,[2] especially as far as its utilization in industrial research is concerned. The possibility of characterizing "porous" systems by means of NMR microscopy was already demonstrated with the determination of pore radii of glass filters[3] and the examination of chromatographic filling materials.[4] We have applied NMR microscopy to open-cell foams; in the example at hand, these are flexible polyurethane foams, which are widely used in upholstery, for example in cars. The use of NMR image data for the characterization of such foams in product development seems attractive in that NMR images are digital and can therefore easily be processed. Thus, it should be possible to reduce the large data set of one image to a few relevant properties in order to correlate these with properties of the product. A fundamental prerequisite is that the attainable spacial resolution is sufficient for the structures of interest.

In NMR imaging, switched magnetic field gradients are used to encode space into frequency.[1] The "spectrum" obtained after a Fourier transformation is the profile of the sample along the direction of the gradient, that is, the projection of the sample on this direction. In the 3D spin echo technique, the three-dimensional image is obtained by using three orthogonal gradients and by processing the data in the same way as in multidimensional NMR spectroscopy.

A special feature of NMR imaging is that the three dimensions are equal in the experiment. Thus, instead of scanning image planes and later extending them to 3D by image stacking (as is the case in laser scan microscopy) 3D information is accumulated immediately. Each accumulation records signals from the complete sample, which means that the advantage of the Fourier technique of a later reduction to the frequency components is used, just as in NMR spectroscopy. After the threefold Fourier transformation, the result of such a measurement is a 3D data matrix in which the signal intensity for each image point ("voxel") can be found.

In polymer foams, the polymer itself cannot be made visible with the necessary resolution of better than 20 μm owing to the width of the ^{1}H signal. Therefore, the foam is filled with a liquid, and then the measurement is made.[2a, 5] The foam structure is obtained upon inversion of the image. Figure 1 shows such a foam image after the last step of processing, the surface reconstruction. The intensity data mentioned can be seen as shades of color in a 2D section in Figure 2. The 3D foam images (Figure 1) give a good visual impression of the foam structure that is intensified by the possibility of image animation on the computer.

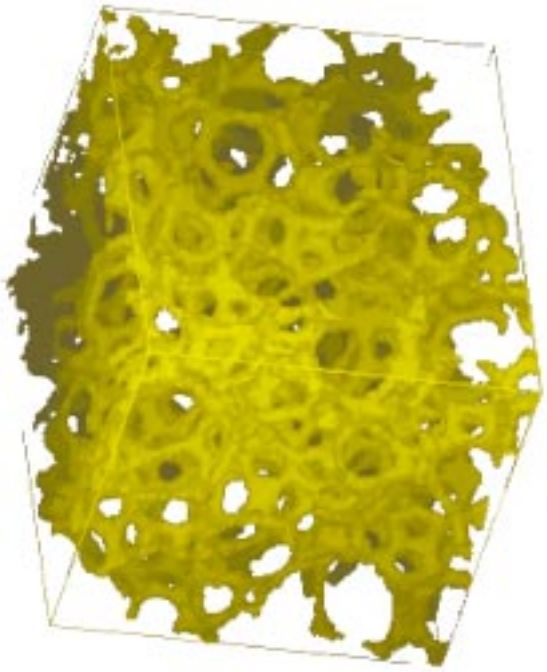

Figure 1. 3D surface reconstruction of a flexible polyurethane foam (inverted image, detail 2 mm × 2 mm × 2 mm, 128^3 of 256^3 image points, resolution 15.6 μm).

Several objectives are possible for further image processing. To judge the quality of the image and the local density of the foam, a statistic of the intensity entries per voxel suggests itself. As is shown in the following, the local density of the foam can also be calculated from such a voxel statistic. The transformation of the cell struts into vectors yields information on the cell geometry.[5] Finally, the distribution of cell diameters can be determined by means of object adjustment. Our results of corresponding evaluation routines concerning voxel statistics and cell diameters are presented in the following.

The image data are available as a series of intensity entries for the individual image points after the Fourier transformation. For the usual echo times of several milliseconds, the polymer signal has decayed completely at the time of detection, so that the signal intensity of the voxel describes the "degree of filling" of the voxel in question with water. The intensity values can be depicted as shades of color in a 2D section, as has been done in Figure 2 for two resolutions (the struts are dark). The cross-section of the struts is only reproduced well at a resolution of 8 μm (edge length of the cubic voxel); however, the poorer resolution (15 μm) is sufficient for a representation of the foam morphology (see Figure 1). The measurement time needed limits the attainable

[*] Dr. R.Voelkel
ZKM G201, Kunststofflaboratorium
BASF AG, D-67056 Ludwigshafen (Germany)
Fax: (+49) 621-60-92281
E-mail: ruediger.voelkel@basf-ag.de
Dr. M. Szayna
National Institutes of Health, Baltimore MD 21234 (USA)
L. Zedler
Gesellschaft für Angewandte Informatik, Berlin (Germany)

  1433-7851/99/3817-2551 $ 17.50+.50/0

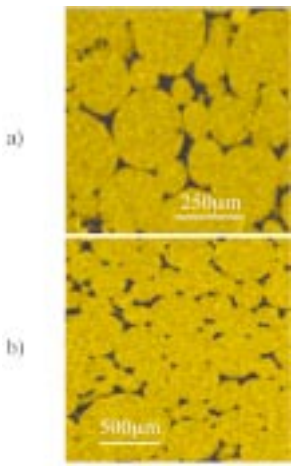

Figure 2. 2D section through a 3D data set (detail). The struts (dark) are only represented correctly at a resolution of 8 µm (above). The resolution of the lower image amounts to 15.6 µm. Complete images 256^3 data points each.

resolution in the imaging of liquids, as an improvement in the resolution by a factor of 2 reduces the volume of the voxel to 1/8, which has to be compensated by a 64-fold measurement time. Besides shorter measurement times, a larger voxel increases the registered image area for the same number of image points, which is advantageous for a statistical evaluation, for example, of the cell size. At present, considerable measurement times are required for a 3D recording with a resolution of 8 µm (typically two to three days); fast imaging sequences common in medicine technology should, however, allow considerable saving of time.

To determine the cell diameters, we use 2D sections from the 3D data set; Figure 2 shows such a section. For the evaluation, the lighter areas inside the cells are filled with ellipses whose boundaries are formed by the darker struts (Figure 3). As all 2D layers are present, a plausibility check is

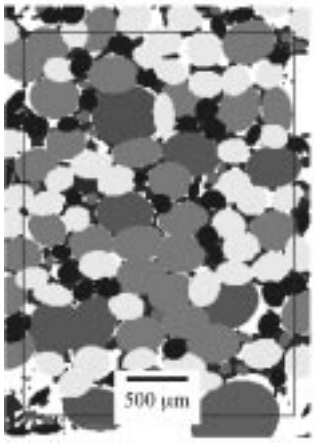

Figure 3. Ellipses fitted to the cells, coding of the areas in shades of grey, resolution 15.6 µm, 256^2 image points per slice.

possible; that is, a large cell must continue in the next layer, a strut cannot end suddenly, etc. Thus, we use the available 3D information although a direct adjustment of ellipsoids to the 3D data was not possible so far owing to lack of software. The 2D adaptation of ellipses leads to a distribution of equivalent cell radii (with the same circular area as the corresponding ellipse), as shown in Figure 4. For control purposes, images made with optical microscopy were evaluated with the same program. The two methods are in accordance with each other (Figure 4).

Histograms with the intensity data (Figure 5 A, curves a and b) are used to judge the quality of the image (signal-to-noise ratio). The values for intensity I are plotted on the abscissa, the number or frequency H with which the value in question occurs on the ordinate. The initial part of the curve is enlarged (Figure 5 A, curve b, right ordinate). The occurring intensity values lie between an empty voxel (no liquid, a "grey level" of 7 units in Figure 5 A) and an image point completely filled with liquid (Figure 5 A, 57 units), and define the dynamic range. In the foam, volume points completely filled with liquid come from the inside of the foam cells and are correspondingly frequent. The spike which is therefore expected (in Figure 5 A at 57 units) is broadend by the noise to a Gaussian line. The ratio of dynamic area (intensity values or "grey" level, respectively; in Figure 5 A the values between 7 and 57) to the width of the Gaussian curve characterizes the signal-to-noise (S/N) ratio of the picture (S/N ≈ 5 in Figure 5). By means of deconvolution with the Gaussian line broadening taken from the water-filled voxels, the intensity histogram can be "de-smeared" (Figure 5 A, curve c). The smeared curve corresponding to this intensity statistic (curve c) is drawn with a dashed line next to curves a and b in Figure 5 A, and it shows good accordance with the experimental values (solid lines).

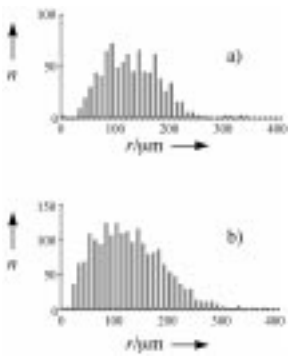

Figure 4. Distribution (number n) of the area-equivalent cell radii r from NMR data and optical microscopy. a) NMR data: resolution 15.6 µm, evaluation of 2×4 layers lying behind each other (each 15.6 µm thick), detail 2.4 mm × 3.2 mm each, together 874 ellipses, mean radius 132 µm (standard deviation $s = 55$ µm). b) Optical microscopy data: three images, each 8.6 mm × 6.6 mm, 1931 ellipses, mean value 130 µm ($s = 66$ µm).

If the resolution is sufficiently good for the description of the structures at hand, all intensity values are approximately equally abundant in the medium dynamic area (Figure 5 A, curves a and b), with an additional local maximum at the intensity value for the "empty" and the "full" image points, especially well discernible in the de-smeared curve (Figure 5 A, resolution 8 µm, curve c). However, if the single image point is of a similar size or larger than the smallest structure, here the connecting junctions of the foam struts, then there are no "empty" voxels any more, and the abundance of partly filled image points increases from the empty to the full image point with the "degree of filling" with liquid (Figure 5 B, resolution 15 µm). In this case the morphology of the foam is correctly represented (Figure 1), but not the cross-section of the single strut (Figure 2, bottom).

An integration of the de-smeared histogram (e.g. Figure 5 B, curve c) weighted with the degree of filling with polymer yields the volume content of the polymer (5.1 %) and can be converted into the local density (5.7 g cm^{-3}).

Residues of the cell membranes are not registered by NMR microscopy since, with their thickness of typically 0.1 µm, they decrease the degree of filling of an image point (size $(8\ \mu m)^3$) otherwise filled with liquid by only about 1 %. This is less than the interval length of typically 2 % in the dynamic range (cf. Figure 5). In other words, an image point contributes to the

  1433-7851/99/3817-2552 $ 17.50+.50/0

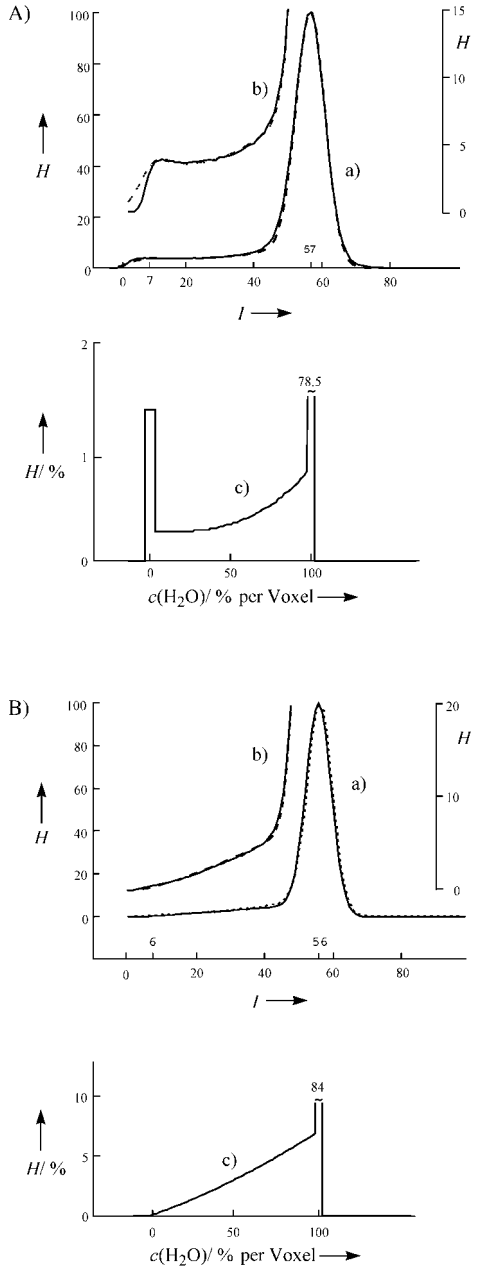

Figure 5. Statistics of the signal intensities in the image points. A: resolution $(8\ \mu m)^3$ per voxel, detail of 128^3 image points (complete image 256^3). B: resolution $(15.6\ \mu m)^3$ per voxel, detail of 144^3 image points (out of 256^3); a) distribution of the voxel intensities (left ordinate); b) enlargement of curve a (right ordinate). Measured data (——) and the adaptations (– – –) are shown, maximum normalized to 100. c) De-smeared distribution, abundance against degree of filling with liquid c [% per voxel] (x axis renormalized).

intensity value "100 % water" after deconvolution, whether it contains cell membranes besides liquid or not. Under these circumstances, NMR microscopy does not register the very thin membrane residues. For a known volume content of the polymer in the foam (i.e. known macroscopic density) this effect could be utilized to determine the proportion of polymer localized in the membranes from the difference between NMR volume content and macroscopic volume content. The amount of material localized in the membranes influences the mechanical behavior of the foam: A foam with membranes shows a higher rigidity and strength in the tension test than a pure struts foam of equal density;[6] the amount of membrane material is therefore an important piece of information for the interpretation of the mechanical data.

Experimental Section

The foams were generated in the laboratory from a polyol based on polypropylene oxide (starter: glycerol, 14 wt % ethylene oxide end caps, $M = 2000$ per OH group), methylene diisocyanate (MDI; mixture of binuclear and polynuclear MDI) with an NCO/OH ratio of 1.0 and with 3.7 wt % water (based on polyol) as foaming agent as well as supplementary agents (cell opener, stabilizer, catalyst). Density of the foam about $50.75\ g\,L^{-1}$, density of the compact polymer $1.12-1.13\ g\,cm^{-3}$. The open-cell foams were evacuated and filled with doped water ($CuSO_4$) or silicon oil.

The images were recorded on a wide-bore Bruker Avance DSX400 NMR instrument with a micro-imaging probe (narrow-bore, gradient max. $3 \times 2\ T\,m^{-1}$). Echo time 4 ms; waiting time 125 ms – 250 ms; gradient $\leq 50\,\%$/1.4 ms (resolution 8 μm), $\leq 60\,\%$/1.9 ms (resolution 15 μm); field of view (FOV) $2 \times 2 \times 2.5\ mm^3$ (resolution 8 μm), $(4\ mm)^3$ (resolution 15 μm), data matrix 256^3 data points; recording time ≤ 72 h. The data processing up to the image was carried out with Paravision (Bruker), the ellipses were adapted with software developed by us (GFaI), and Mathcad was used for the voxel statistics.

Received: December 4, 1998
Revised version: May 20, 1999 [Z12748IE]
German version: *Angew. Chem.* **1999**, *111*, 2709 – 2712

Keywords: foams · materials science · microscopy · NMR spectroscopy · polyurethane

[1] W. Kuhn, *Angew. Chem.* **1990**, *102*, 1 – 20; *Angew. Chem. Int. Ed. Engl.* **1990**, *29*, 1 – 19.
[2] a) *Magnetic Resonance Microscopy* (Eds.: B. Blümich, W. Kuhn), VCH, Weinheim, **1992**, Chap. 2; b) *Spatially Resolved Magnetic Resonance* (Eds.: P. Blümler, P. Blümich, R. Botto, E. Fukushima), WILEY-VCH, Weinheim, **1998.**
[3] J. Pauli, G. Scheying, C. Mügge, A. Zunschke, P. Lorenz, *Fresenius J. Anal. Chem.* **1997**, *357*, 508 – 513.
[4] E. Bayer, W. Müller, M. Ilg, K. Albert, *Angew. Chem.* **1989**, *101*, 1033 – 1035; *Angew. Chem. Int. Ed. Engl.* **1989**, *28*, 1029 – 1032.
[5] a) K. Kose, *J. Magn. Reson. A* **1996**, *118*, 195 – 201; b) K. Kashiwagi, K. Kose, *NMR Biomed.* **1997**, *10*, 13 – 17.
[6] L. J.Gibson, M. F. Ashby, *Cellular solids: structure & properties*, 2nd ed., Cambridge Universitay Press, Cambridge, **1997**, Chap. 5.

  1433-7851/99/3817-2553 $ 17.50+.50/0